Neutrino cross section measurements at MINERνA

F.D. Snider[*] **Fermilab**[†] **E-mail:** rs@fnal.gov

on behalf of the MINERνA Collaboration

The MINERνA experiment is designed to perform detailed studies of neutrino and anti-neutrino interactions with nuclie in the energy range 1 – 10 GeV. In this paper, we present the status of charged-current inclusive and charged-current quasi-elastic cross section measurements for neutrinos, and a preliminary measurement of the charged-current quasi-elastic cross section for anti-neutrinos. The results are based upon an analysis of about 25% of the data taken through July of 2012.

---

[*]Speaker.

1. Introduction

A detailed understanding of neutrino interactions with nuclei underpins two broad and rich areas of research, the study of neutrino properties and nucleon structure. The current generation of neutrino oscillation experiments, for instance, requires a precise measurement of the neutrino-nucleus interaction cross section in the 1–10 GeV energy range. The cross section in this region, however, is poorly measured [1], and the underlying processes that contribute are changing rapidly with energy. Similarly, the energy dependence and role of nuclear effects and final state interactions in quasi-elastic interactions, which are particularly important in oscillation measurements, is not understood [2].

While cross section measurements are essential for the exploration of neutrino properties, there is an equally compelling interest in neutrinos in the study of nuclean structure. Many questions of nucleon structure, such as flavor-dependent structure functions, can be addressed only via studies with neutrinos. As weakly interacting particles, neutrinos offer an important and unique probe into the structure of the nucleon in the nuclear environment.

In this paper, we present the current status of neutrino-nucleus cross section measurements made at the MINERvA experiment [3] at Fermilab. The MINERvA experiment uses a finely segmented scintillating strip detector designed to study neutrino-nucleus and anti-neutrino-nucleus interactions in unprecedented detail. The results presented here represent the analysis of approximately 25% of a dataset collected during beam exposures of 4.0×10^{20} protons-on-target (POT) in neutrino-mode, and 1.7×10^{20} POT in anti-neutrino mode.

After a brief discussion of the neutrino beam, neutrino flux measurement, and the MINERvA detector, we present preliminary results from neutrino charged-current (CC) inclusive, neutrino CC quasi-elastic (CCQE), and anti-neutrino CCQE cross section measurements.

1.1 NuMI beam line

The neutrinos used by MINERvA are created in the Neutrinos at the Main Injector (NuMI) beam line at Fermilab [4] with 120 GeV protons incident on a carbon target. The beam deposits approximately 35×10^{12} POT at a frequency of 0.5 Hz. Two magnetic horns downstream of the target focus secondary π^+ and K^+ (or π^- and K^-) particles into a decay pipe, where they decay to produce neutrinos (anti-neutrinos). Muon monitors embedded in the rock downstream of the decay pipe can be used to augment the flux determination.

The energy spectrum of the neutrino beam can be adjusted by moving the target and magnetic horns. MINERvA has just completed running in a "low-energy" configuration, where the peak of the energy spectrum is about 3 GeV. We estimate the neutrino flux (Fig. 1) using NA49 data to re-weight a QGSP hadron production model in a GEANT4 simulation of the beam and target. The uncertainty in the estimate is approximately 15–16% up to neutrino energies of about 20 GeV, and is dominated by the uncertainty in tertiary hadron production in the target assembly and, for some energies, in beam focusing uncertainties. We expect significant reductions in these uncertainties with improvements to the hadron production model, the use of muon monitor data in the flux estimate, and, if available, new hadron production data.

In the spring of 2013, we will begin data taking with a beam two times more intense and in a "medium energy" configuration, where the peak energy is about 5 GeV.
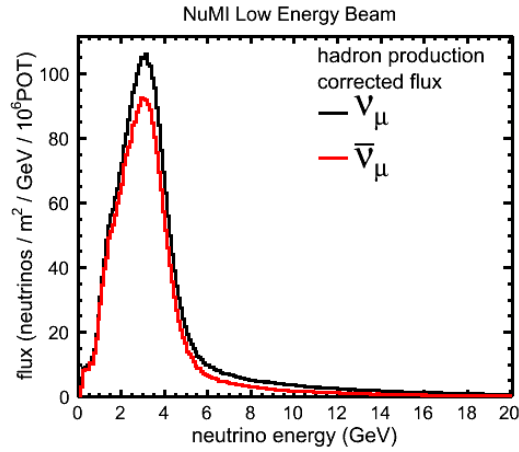
Figure 1: Neutrino (black) and anti-neutrino (red) flux estimated from GEANT4 calculation corrected for hadron production using NA49 data.

1.2 The MINERvA detector

The central part of the MINERvA detector consists of 120 stacked, hexagonal modules 3.45 m across, most of which contain a 2.14 m core with two planes of scintillating strips. Some of the modules in the most upstream portion of the detector substitute various nuclear targets (C, Pb, Fe) for the scintillating strips. Downstream of the nuclear target region is a fully active, finely-segmented tracker. Both the nuclear target and tracker regions are surrounded by electromagnetic and hadronic calorimeters. Additional electromagnetic and hadronic calorimeters lie downstream of the tracker.

A liquid helium target is located immediately upstream of the central detector. Walls of veto scintillators and steel in front of the LHe target help reduce background from muons produced upstream.

The MINOS near detector [5], located immediately downstream of the MINERvA central detector, is used as a spectrometer for muons that exit the rear of MINERvA.
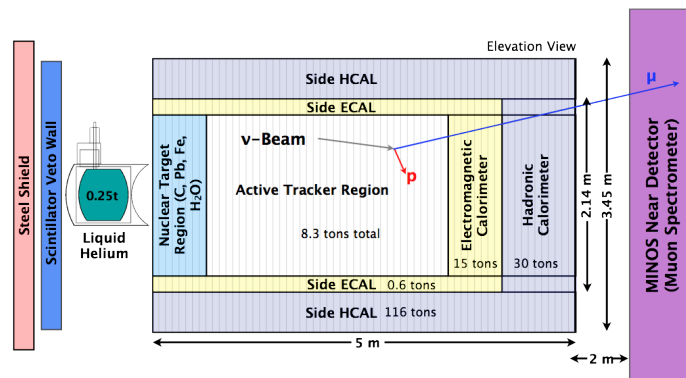

Figure 2: The MINERvA detector.

2. Neutrino charged current inclusive analysis

The neutrino CC inclusive analysis will measure the cross section for events consistent with any neutrino interaction that produces a final state muon. To isolate these interactions, we select events wth a single muon candidate in MINERvA that is matched to a muon track in MINOS, and a reconstructed interaction vertex within the fiducial volume of the detector. We then measure the recoil energy by summing over the observed energy in all tracks (excluding the muon candidate), showers, and isolated energy deposits in the tracker and EM calorimeter.

Requiring a match between the muon track in the central MINERvA detector and the MINOS spectrometer limits the angular acceptance to scattering angles below 10°–20°, and the minimum neutrino energy to about 2 GeV. At the time of writing, the analysis has measured the muon angle, muon energy, recoil energy, and reconstructed neutrino energy distributions, all normalized to the number of POT. Figure 3 shows the muon scattering angle distribution compared to a GENIE [6] MC prediction, with full statistical and systematic uncertainties.
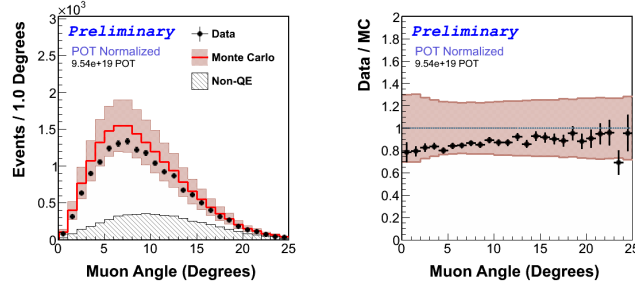

Figure 3: Left: measured POT-normalized muon scattering angle for neutrino CC inclusive events compared to MC prediction. Right: the ratio of data to the MC prediction.

3. Neutrino charged-current quasi-elastic analysis

In neutrino CCQE interactions, the neutrino scatters coherently off a single neutron producing a muon and a single proton in the final state. Assuming no final-state interactions, we can use two-body kinematics to infer the incoming neutrino energy E_ν and the Q^2 of the interaction from the scattering angle (θ_μ) and momentum (p_μ) of the out-going muon:

$$E_\nu = \frac{m_\mu^2 - (m_p - E_b)^2 - m_\mu^2 + 2(m_p - E_b)E_\mu}{2(m_p - E_b - E_\mu + p_\mu \cos\theta_\mu)}, \tag{3.1}$$

$$Q^2 = 2E_\nu(E_\mu - p_\mu \cos\theta_\mu) - m_\mu^2, \tag{3.2}$$

where E_b is the nuclear binding energy of the proton, and m_μ and m_p are the muon and proton masses, respectively.

To isolate quasi-elastic interactions, we again begin by requiring a single muon track candidate that is matched to a muon track in the MINOS detector. The interaction vertex, which is assumed to be the start of the muon track, is required to be within the fiducial volume of the detector.

Muons produced in material upstream of the interaction vertex can mimic those from quasi-elastic interactions if they traverse strips that have been momentarily inactivated by the data acquisition system due to prior activity in the detector. We eliminate this background by requiring no inactive strips along the muon trajectory in the four planes immediately upstream of the interaction vertex. We then require at most one other track associated with the muon vertex. Finally, since CCQE events have relatively small recoil energies, we demand that the recoil energy, excluding that within a 10 cm sphere around the interaction vertex, is less than a Q^2-dependent maximum.

We have currently measured POT-normalized kinematic distributions for the events passing these selection criteria. Figure 4, for instance, shows the measured distribution of reconstructed Q^2_{QE} compared to MC in two bins of incident neutrino energy, 2.0 to 4.0 GeV, and 4.0 to 10.0 GeV, where the uncertainties include both statistical and systematic contributions. We expect to reduce uncertainties and complete the cross section measurement in the near future.
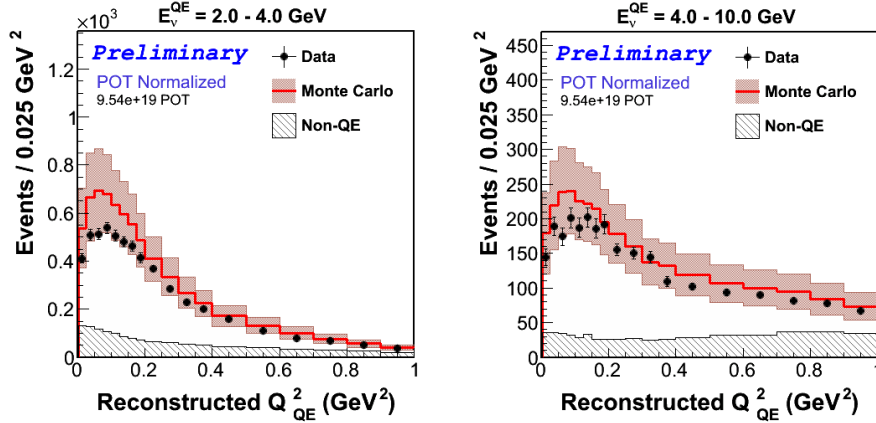

Figure 4: Reconstructed Q^2_{QE} distributions compared to MC in two slices of neutrino energy.

4. Anti-neutrino charged-current quasi-elastic cross section

In anti-neutrino CCEQ interactions, the incoming anti-neutrino interacts with a single proton in a nucleus producing a μ^+ and a neutron in the final state. Rather than a muon candidate and a track as in neutrino CCQE events, anti-neutrino CCQE events have a μ^+ candidate and an area of energy deposition where the neutron interacts in the detector. The neutron shower is typically displaced from the anti-neutrino interaction vertex. The event selection therefore requires a single muon candidate track that is matched to a μ^+ track //in MINOS (with the same background muon rejection criteria as used in the neutrino CCQE analysis), a reconstructed vertex (taken as the start of the μ track) within the fiducial volume of the detector, and no more than one region of shower activity in the detector. To isolate the signal from the dominant non-CCQE background, we again require that the sum of recoil energy farther than 10 cm from the vertex is less than a Q^2-dependent maximum. Finally, we require the anti-neutrino energy to be less than 10 GeV, where we use Eq. 3.1 to estimate the energy of the anti-neutrino. The measured distributions of anti-neutrino energy and Q^2 are shown in Fig. 5

To subtract non-CCQE neutrino and anti-neutrino interaction background, we fit the recoil energy distribution in bins of reconstructed Q^2 to shape templates for background determined using MC. The background is less than about 20% across the entire Q^2 range.

Next, we unfold resolution effects on the measured Q^2 distribution to obtain an estimate of the true Q^2 distribution using a simple matrix inversion method, where we use MC to calculate the smearing matrix. Each element M_{ij} of the matrix is the fraction of events with a true Q^2 in bin j that is measured to be in bin i. The diagonal elements vary between about 0.9 in the lowest bin of Q^2 to about 0.5 in the highest.

We then correct the unfolded distribution for efficiency and acceptance as estimated from MC. The product of efficiency times acceptance varies from about 0.65 at low Q^2 to about 0.13 for Q^2 around 1.65 GeV^2.

Finally, we extract the cross section (Fig. 6) by dividing by the flux, calculated as described in Sect. 1.1. In the left plot in Fig. 6, we compare the measured differential cross section as a function of Q^2 with a GENIE prediction. The right plot shows the systematic uncertainties as a function of Q^2. The uncertainties are estimated by repeatedly varying the inputs according to their uncertainties and re-running the analysis, then extracting overall uncertainty bands from the ensemble of results. The flux dominates the systematic uncertainty in most bins of Q^2, except in the last, where the muon energy uncertainty dominates. We expect sigificant reductions in these uncertainties with further analysis.
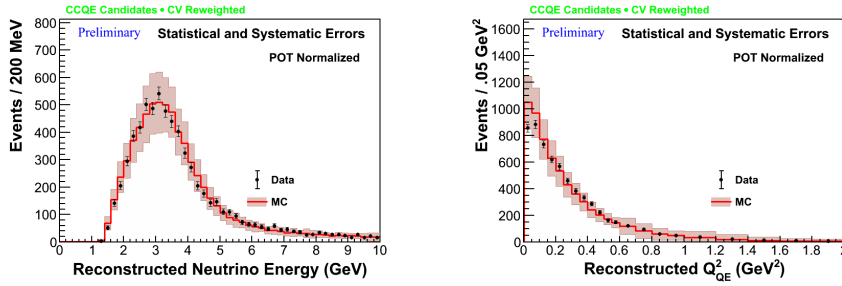

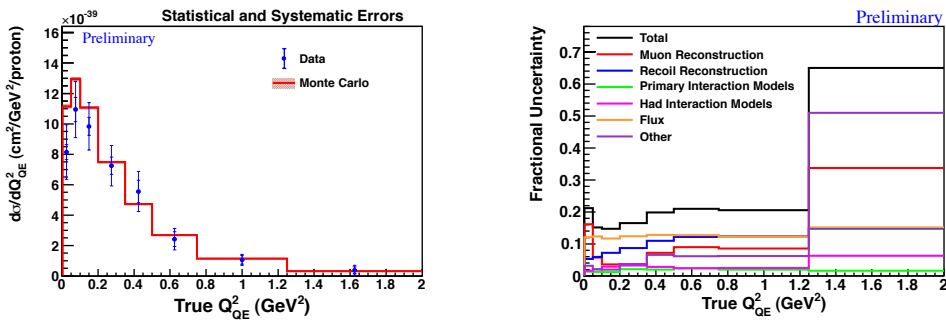**Figure 5:** Anti-neutrino CCQE reconstructed netrino energy and Q^2.

Figure 6: Left: Anti-neutrino CCQE cross section. (MC = GENIE 2.6.4, M_A = 0.99 GeV/c2, RFG, Pauli-blocking, no meson exchange currents.) Right: contributions to the systematic uncertainty.
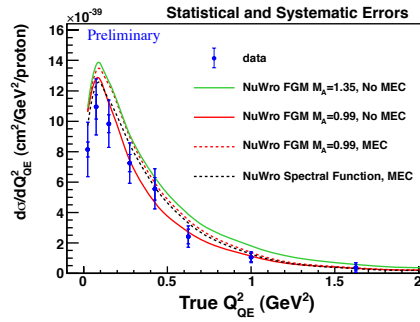
Figure 7: Anti-neutrino CCQE cross section compared to NuWro prediction under various model and meson exchange current assumptions.

An interesting question in quasi-elastic interactions is the extent to which meson exchange currents (MEC) contribute to the cross section. The NuWro program [7] includes these contributions; we compare our data to NuWro predictions in Fig 7. With further analysis and the addition of the remaining 75% of the data recorded to date, we expect to be able to make definitive statements regarding the role of MEC contributions.

5. Summary

The MINERvA experiment has recently concluded neutrino and anti-neutrino runs in a low energy beam configuration. Preliminary results from this run presented here include kinematic distributions in neutrino CC inclusive and neutrino CCQE analyses, and a preliminary measurement of the anti-neutrino CCQE differential cross section as a function of Q^2. The analyses used approximately 25% of the data that has been accumulated to date. We expect dramatic reductions in statistical and many systematic uncertainties as we analyze the balance of the dataset and continue to improve the analyses. Preliminary results on the the ratio of neutrino CC inclusive cross section in iron and lead, are also available and were presented in the poster session of this conference.

References

[1] See, for instance, J.A. Formaggio and G.P. Zeller, Rev. Mod. Phys. **84**, 1307 (2012).

[2] A. A. Aguilar-Arevalo *et al.* [MiniBooNE Collaboration], Phys. Rev. D **81**, 092005 (2010)

[3] D. Drakoulakos *et al.* [Minerva Collaboration], hep-ex/0405002.

[4] K. Anderson *et al.*, Tech. Rep., FERMILAB-DESIGN-1998-01, Fermi National Accelerator Laboratory (1998); S. E. Kopp, Proc. 2005 IEEE Particle Accel. Conference (2005), arXiv:physics/0508001.

[5] See D. G. Michael *et al.*, Nucl. Instrum. Meth. A **596**, 190 (2008). and references therein.

[6] C. Andreopoulos, *et al.*, Nucl. Instrum. Meth. A **614**, 87 (2010)

[7] See \http://bor.ift.uniwroc.pl/nuwro/, C. Juszczak, J.A. Nowak and J.T. Sobczyk, Nucl. Phys. B (Proc. Suppl) 159, 211 (006).